Marked *Neurospora crassa* strains for competition experiments and Bayesian methods for fitness estimates

Ilkka Kronholm[*], Tereza Ormsby[†,‡], Kevin J. McNaught[†], Eric U. Selker[†], Tarmo Ketola[*]

[*]Department of Biological and Environmental Sciences, University of Jyväskylä, FI-40014 Jyväskylä, Finland

[†]Institute of Molecular Biology, University of Oregon, Eugene, United States

[‡]Current address: Institute of Organic Chemistry and Biochemistry of the Czech Academy of Sciences, 16610 Prague 6, Czech Republic

Running Head: Competition experiments with *Neurospora*

Keywords: fungi, high resolution melting, competitive fitness, experimental evolution

Corresponding author:

Ilkka Kronholm

Department of Biological and Environmental Sciences,

University of Jyväskylä,

P.O. Box 35, FI-40014

Jyväskylä,

Finland

Fax +358 14 617 239

Email: ilkka.kronholm@jyu.fi

Abstract

The filamentous fungus *Neurospora crassa*, a model microbial eukaryote, has a life cycle with many features that make it suitable for studying experimental evolution. However, it has lacked a general tool for estimating relative fitness of different strains in competition experiments. To remedy this need, we constructed *N. crassa* strains that contain a modified *csr-1* locus and developed an assay for detecting the proportion of the marked strain using a post PCR high resolution melting assay. DNA extraction from spore samples can be performed on 96-well plates, followed by a PCR step, which allows many samples to be processed with ease. Furthermore, we suggest a Bayesian approach for estimating relative fitness from competition experiments that takes into account the uncertainty in measured strain proportions. We show that when combining all available information from different experiments the *csr-1** allele has no detectable fitness effect, which makes it a suitable marker for competition experiments. However, there was an effect of the mating type locus, as mating type *mat a* has a higher fitness than *mat A*. As a proof of concept, we estimate the fitness effect of the *qde-2* mutation, a gene in the RNA interference pathway, and show that its competitive fitness is lower than what would be expected from its mycelial growth rate alone.

Introduction

The filamentous fungus *Neurospora crassa* is a model eukaryote with a wealth of genetic resources (ROCHE *et al.*, 2014; MCCLUSKEY *et al.*, 2010; COLOT *et al.*, 2006), and many aspects of its cellular and molecular biology have been intensively studied (ROCHE *et al.*, 2014). There is now a great deal of interest to study evolution of *Neurospora* and other filamentous fungi experimentally (LEE and DIGHTON, 2010; GRAHAM *et al.*, 2014; ROMERO-OLIVARES *et al.*, 2015; BASTIAANS *et al.*, 2016; FISHER and LANG, 2016; MEUNIER *et al.*, 2018). Despite having many beneficial characteristics for experimental evolution studies, *N. crassa* has lagged somewhat behind unicellular microbes in this area, as methodology for measuring competitive fitness has been missing.

Studying evolution of filamentous fungi is challenging because it is not clear how to define fitness in filamentous organisms (PRINGLE and TAYLOR, 2002). Many fungi have complicated life cycles, and individuals can be hard to define, complicating the choice of the appropriate fitness metric (PRINGLE and TAYLOR, 2002; GILCHRIST *et al.*, 2006). Moreover, individual fitness components, such as mycelial growth rate or conidial (asexual spore) production, are not necessarily strongly correlated with each other (ANDERSON *et al.*, 2018). Yet, modeling results have shown that for saprotrophic fungi that colonize discrete resource patches, such as *N. crassa*, spore production is the critical fitness component (GILCHRIST *et al.*, 2006). While different experimental evolution protocols have been used for filamentous fungi, it has been shown that transferring spores to the next generation leads to the greatest response to selection (SCHOUSTRA *et al.*, 2005). Accordingly, one should measure fitness in conditions that correspond to the propagation conditions. Therefore, spore production is often the measure of interest. However, just comparing spore production of two different genotypes does not necessarily predict which of the genotypes would prevail when the two are competing against one another. From studies with bacteria, we know that predicting the winner of two competing genotypes from their individual characteristics is difficult, and the best method is to measure competitive fitness directly (LENSKI *et al.*, 1998).

To measure competitive fitness, one genotype needs to be tested against another, often the ancestor, and the proportions of these genotypes in culture need to be followed. This requires

that the genotypes are distinguishable. In controlled experiments, a morphological marker has undesirable fitness consequences, and often the genetic changes that happened between ancestor and derived genotypes are not fully known. Therefore, an engineered genetic marker is desirable. Some previous functional studies have used strains that express a fusion protein of histone H1 and green fluorescent protein to distinguish nuclei (FREITAG *et al.*, 2004) and different fluorescent labels could be used to distinguish between different strains. While this approach is necessary for many functional studies, it requires imaging with a fluorescent microscope and counting of individual nuclei, which can be laborious in large evolution experiments. At the moment, a system to easily estimate competitive fitness of *N. crassa* comparable to the *ara* marker in *Escherichia coli* (LENSKI *et al.*, 1998) does not exist.

To address this lack of suitably marked strains, we constructed genetically marked strains of *N. crassa*, and developed a PCR-based method to assess marker frequency in a sample of conidia. We used a high resolution melting (HRM) assay to distinguish between the amplification products of marked and wild type strains. HRM is a method in which a real-time PCR machine is used to monitor melting of PCR products. A fluorescent dye that binds double stranded DNA is included; when temperature increases, melting of the PCR products is monitored as the decrease in fluorescence caused by DNA strand separation. Sequence differences between different alleles cause their melting curves to differ, which can be used to distinguish them (WITTWER *et al.*, 2003). By comparing unknown samples to known standards, the relative proportions of the different alleles can be determined. However, as with any other biochemical assay based on standard curves, there is some uncertainty associated with the standard curve and the samples. Therefore, we suggest a Bayesian statistical model to estimate fitness effects from competition experiments which incorporates all the uncertainty associated with our measurements. HRM has been previously used in several different applications, including genotyping (WITTWER *et al.*, 2003), identification of different fungal species (ARANCIA *et al.*, 2011), methylation analysis (WOJDACZ and DOBROVIC, 2007), and quantification of relative amounts of different bacterial strains in a sample to study competition (ASHRAFI *et al.*, 2017).

We show that our marked strain can be used in competition experiments, and that the HRM assay discriminates between the marked and the wild type strains. We further demonstrate that the marker itself does not have any large fitness effect and illustrate the utility of our method by estimating competitive fitness effects for the different mating type idiomorphs, and for a mutant in the RNA interference pathway, *qde-2*.

Materials and methods

Neurospora crassa strains and culture methods

We used the nearly isogenic laboratory strains FGSC 2489 and 4200, obtained from the Fungal Genetics Stock Center (McCluskey *et al.*, 2010), to generate a uniform genetic background. We backcrossed 4200 to 2489, always picking *mat a* offspring. Previously, we had performed five backcross generations (Kronholm *et al.*, 2016), and now we performed further backcrosses until generation nine (BC_9). From BC_9 offspring we picked *mat A* and *mat a* genotypes to obtain BC_9 2489 *mat A* and BC_9 2489 *mat a*. Same backcrossing was done for *qde-2* mutant to obtain BC_9 2489 *mat A*; Δ*qde-2* and BC_9 2489 *mat a*; Δ*qde-2*. All strains used in this study, including the marked strains described below, are shown in Table 1. Hereafter we will refer to the BC_9 2489 background simply as 2489.

We used standard laboratory protocols to culture *N. crassa* (Davis and de Serres, 1970). Growth medium was Vogel's medium N (Metzenberg, 2003) with 1.5% agar. Strains were grown in Lab companion ILP-02/12 (Jeio Tech, South Korea) growth chambers at 25 °C unless otherwise noted.

Construction of marked strains

Mutations in the *csr-1* gene cause resistance to the drug cyclosporin A (Bardiya and Shiu, 2007). This allows the use of homologous recombination in *N. crassa* strains without disabled non-homologous end-joining DNA repair pathway (Ninomiya *et al.*, 2004).

Table 1: Strains used in this study. Strain ID shows either FGSC ID number or identifier. Strains with genotype BC_9 2489 have the same genetic background generated by backcrossing 4200 nine times to 2489. FGSC = Fungal Genetics Stock Center, *wt* = wild type.

Strain ID	Genotype	Source
2489	*wt mat A*	FGSC
4200	*wt mat a*	FGSC
K13	BC_9 2489 *mat A*	This study
K14	BC_9 2489 *mat a*	This study
K15	BC_9 2489 *mat A csr-1**	This study
K16	BC_9 2489 *mat a csr-1**	This study
K17	BC_9 2489 *mat A*; Δ*qde-2*	This study
K18	BC_9 2489 *mat a*; Δ*qde-2*	This study
K19	BC_9 2489 *mat A csr-1**; Δ*qde-2*	This study
K20	BC_9 2489 *mat a csr-1**; Δ*qde-2*	This study

Making the *csr-1** construct

The overall strategy for making the construct used for transformation by PCR-stitching is illustrated in Figure 1. We made a linear construct that was homologous to *csr-1*, except that it contained a modified sequence (`ATCCGAATTCATGTAATAGTGT`), which introduces an EcoRI restriction site (`GAATTC`), two early stop codons, `TAA` and `TAG`, and single base pair deletion causing a frameshift (Figure 1). The *csr-1* gene is on chromosome 1, between coordinates 7403946–7406381 on the reverse strand, while the modified sequence is located between coordinates 7405193–7405212 (*N. crassa* genome assembly NC12). We modified this part of the *csr-1* sequence because the `ATG` it contains is the initiation codon for the cytosolic isoform of the protein. A mitochondrial isoform is initiated from an alternative start upstream, and we wanted to abolish the function of *csr-1* completely.

To make the construct, we amplified two flanking 1 kb regions with primers such that one of the primers contained a tail with the new modified sequence and a region that was homologous to the other PCR-product (Figure 1). We used primers csrL-f and csrL-r to amplify the left flanking region and primers csrR-f and csrR-r to amplify the right flanking region (all primer sequences are given in Table S1). These products were amplified with the Phusion DNA polymerase (Thermo Scientific) in a 50 µl PCR reaction containing: 1 $\times$ HF-buffer, 0.2 mM each dNTP, 0.25 µM each

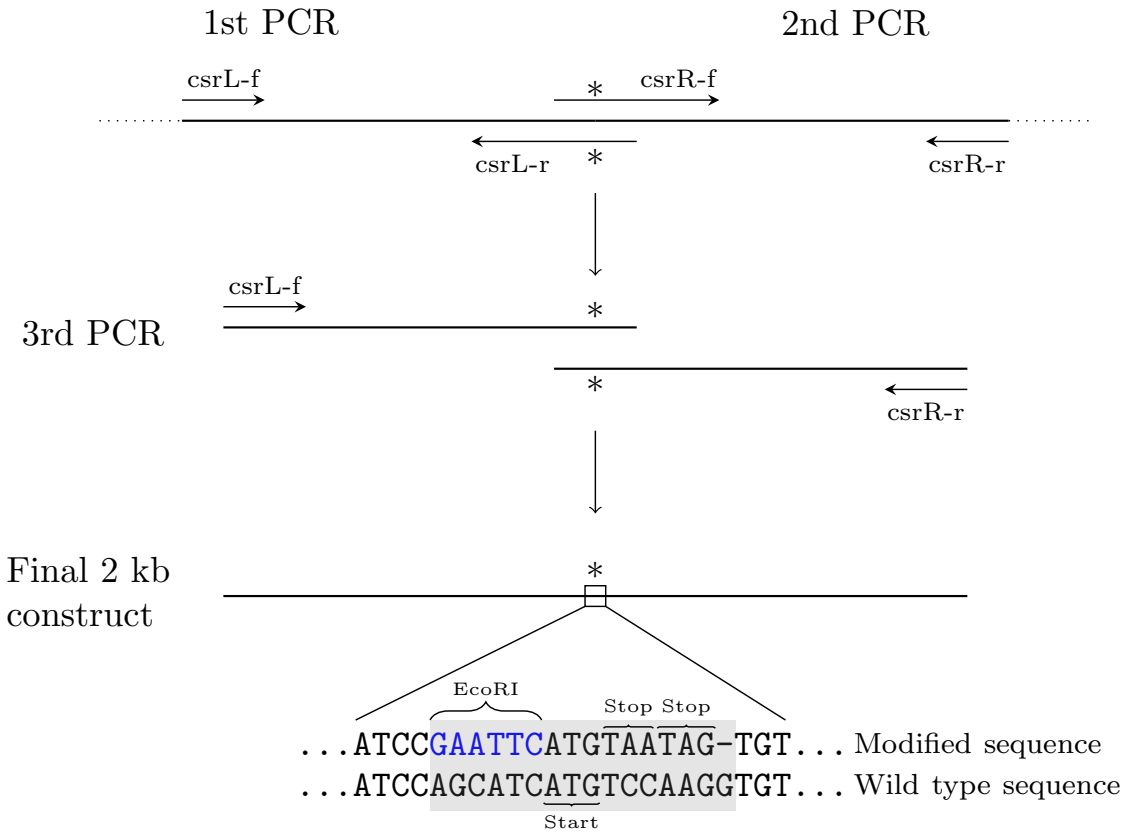

Figure 1: Overall strategy for generating the final construct by PCR-stitching. Primer names correspond to names in table S1.

primer, 100 ng of DNA, and 0.4 U of Phusion DNA polymerase. Reaction conditions for both reactions were: 1 min at 98 °C, then 30 cycles of 98 °C for 10 s, 60 °C for 30 s, 72 °C for 30 s, and a final extension at 72 °C for 5 min. PCR reactions were loaded on a 0.8% agarose gel and the 1 kb bands were extracted from the gel, and cleaned using GenCatch gel extraction kit (Epoch Life Science) according to the manufacturer's instructions.

The final stitching PCR was performed using primers csrL-f and csrR-r with LA Taq polymerase (Takara) in a 50 µl reaction. The reaction contained: 1× LA PCR buffer, 0.4 mM each dNTP, 2 µl of both csrL and csrR templates, 0.2 µM each primer, and 25 U of LA Taq. Reaction conditions were: 94 °C for 1 min, followed by 35 cycles of 98 °C 10 s, 68 °C 5 min, and final extension at 72 °C for 10 min. The PCR reaction was loaded on a 0.8% agarose gel, and the 2 kb band was extracted and purified as described above.

Transformation

We transformed the strain BC_9 2489 *mat A* by electroporation following MARGOLIN *et al.* (1997). For electroporation, we mixed 200 ng of the construct and 40 µl of electrocompetent conidia in a chilled electroporation cuvette (2 mm gap), incubated on ice for 5 min, and electroporated with settings of: 600 Ω, 25 µF, and 1.5 kV. Immediately after electroporation 950 µl of ice cold 1 M sorbitol was added to the cuvette and mixed.

Electroporated conidia were then transferred to a 50 ml conical tube with 9 ml of 32 °C liquid medium without sucrose, and incubated with shaking for 2 h at 32 °C. After the incubation, 10 ml of molten 2×top-agar (standard growth medium with 2% agar, 2 M sorbitol, and 10 µg/ml cyclosporin A) was added to the culture and poured immediately on to selective medium (normal growth medium with 1.5% agar and 5 µg/ml cyclosporin A). Cyclosporin A was dissolved in EtOH and added after autoclaving. Plates were incubated until colonies were visible, which were then picked and kept on slants.

Validation of strains

To confirm transformants, we screened candidates by PCR with csrL-f and csrR-r primers and EcoRI digestion to identify strains containing the modified sequence. We grew mycelia for each of the colonies in a 5 ml liquid culture for 2 days in shaking at 32 °C and harvested the mycelium, tissue was then lyophilized and pulverized. Then we extracted DNA by a protocol adapted from OAKLEY *et al.* (1987). The original protocol was changed so that 1 ml of TCA/EtOH was used, and precipitation was done at −20 °C for 1 h. In addition after incubation with RNase A solution (containing 0.15 mg/ml RNAse A), samples were extracted once with chloroform: 200 µl of chloroform was added, samples were vortexed, and centrifuged for 5 min at 14 000 rpm. Supernatant was transferred to a new tube, and 900 µL of 8:1 isopropanol:7.5 M NH_4OAc solution was added. Samples were mixed and centrifuges for 1 min, and supernatant was discarded. Pellet was washed once with 70% ethanol and air dried, and then resuspended in TE-buffer. 25 µl PCR reactions were performed using Phusion DNA polymerase as above with primers csrL-f and csrR-r. Cultures whose PCR product was digested with EcoRI were kept for further analysis. Sanger sequencing of positive transformants was done using standard protocols.

A positive transformant, 2489 *mat A csr-1**, was crossed to strain 2489 *mat a* to obtain 2489 *mat a csr-1**. Then 2489 *mat A*; Δ*qde-2* was crossed to 2489 *mat a csr-1** to obtain genotypes that were *csr-1**; Δ*qde-2* for both mating type idiomorphs. Progeny were screened by PCR using the high resolution melting assay for *csr-1* and PCR-protocol for *mat* locus and *qde-2* as in KRONHOLM *et al.* (2016).

High resolution melting PCR

A high resolution melting (HRM) PCR assay of the *csr-1* gene was developed using primers (csr-hrm-f and csr-hrm-r, Table S1) that amplified a 100 bp PCR product containing the modified sequence. We amplified the product in 10 µl reactions containing 1×Precision melt supermix (Bio-Rad), 200 nM of each primer, and 2 µl of DNA. Sanger sequencing of the PCR product with primers csr-hrm-f and csr-hrm-r confirmed that the correct target was amplified. For HRM analysis, DNA

was extracted by combining 40 µl of conidial suspension and 10 µl of extraction buffer (100 parts of 50 mM Tris pH 8 and two parts of 0.5 M EDTA pH 8.5) and incubating the mixture for 10 min at 98 °C in a PCR machine as in KRONHOLM *et al.* (2016). Same batch of buffer was used for all samples. PCR amplification was performed with a Bio-Rad CFX-96 Real-Time System PCR machine. The reaction conditions were: initial denaturation of 95 °C for 2 min, 40 cycles of 95 °C for 10 s, 60 °C for 30 s, and 72 °C for 30 s. Amplification was followed by a melting curve analysis: initial denaturation phase of 95 °C for 30 s and renaturation at 70 °C for 1 min, followed by a melt curve measurement from 70–90 °C by 0.1 °C intervals for 5 s. Fluorescence was monitored on the SYBR channel.

To construct standard curves for conidial mixtures that contained different known proportions of *csr-1** conidia, we grew the strains 2489 *mat A csr-1**, 2489 *mat a csr-1**, 2489 *mat A*, and 2489 *mat a* for 5 days on slants, and suspended the conidia in 1 ml of 0.01% Tween-80. We then measured conidial concentrations using a CASY TT cell counter (Roche) with a 45 µm capillary and a gating size range from 2.5 µm to 10 µm. We standardized concentrations to 10^8 conidia/ml and combined different proportions of *csr-1*$^+$ and *csr-1** conidia in 40 µl samples with proportions of *csr-1** conidia ranging from 1 to 0 by 0.1 decrements. We also tested a dilution series of conidia (from 10^8 to 10^4 conidia/ml) to asses the effect of starting concentration on HRM results. Competition experiment samples were run on 96-well PCR plates. To control for variation in PCR reaction conditions, we included two independently constructed standard curves on each plate, a no template control, and additional controls of pure *csr-1*$^+$ and *csr-1** conidia.

Competition experiments

Effect of mating type and *csr-1**

The first competition experiment had a full factorial design, in terms of *mat A*, *mat a*, *csr-1*$^+$, and *csr-1**, giving four strain combinations. We measured conidial concentrations as above, and standardized concentrations to 1×10^7 conidia/ml. The experiment was started with 10^5 conidia of both strains in a 75 × 25 mm test tube containing 1 ml of slanted agar medium. Each competition had

five replicate populations, giving a total of 20 populations. Strains in the competition experiments were transferred every four or five days for three transfers. For a transfer, the conidia produced in a tube were suspended in 1 ml of 0.01% Tween-80 and 50 µl of conidial suspensions were transferred to new tubes. At each transfer, 40 µl of conidial suspension was taken for DNA extraction.

Fitness effect of the *qde-2* mutation

In the second competition experiment we used four strain combinations, so that only strains with different mating types were competed and competing strains always differed from each other with respect to the other loci. Five replicate populations for each different strain combination were used, giving 20 populations in total. Competitions were performed as described above, but at 35 °C.

Statistical analyses

All statistical analysis and data processing were done using the R environment version 3.5.2 (R CORE TEAM, 2018). For Bayesian analyses we used the Stan language (CARPENTER *et al.*, 2017), that implements adaptive Hamiltonian Monte Carlo sampling. Stan was interfaced by the R package 'rethinking' (MCELREATH, 2015). For plotting we used the 'ggplot2' R package (WICKHAM, 2016).

Estimation of *csr-1** allele proportion

To process the melting curve data, we followed the approach used by ASHRAFI *et al.* (2017) with some modifications. We first normalized the fluorescence data (RFU) between 0 and 1. The melting temperature for a given sample, i.e. temperature of the inflection point of its melting curve, was found based on the maximum of the spline interpolation of the negative first derivative of the melting curve. We also calculated the difference curve for the normalized RFU data, we subtracted RFU of the positive control of *csr-1** from the RFU of each sample. For further analysis using the normalized RFU differences, we used the temperature that gave the maximal differences between standard curve samples.

To estimate the proportion of conidia that contain the *csr-1** allele, we first built a standard curve and then estimated the proportion in unknown samples using this curve. For estimating the standard curve, we used the approach recommended by ASHRAFI *et al.* (2017): the model was $y = a + Bx$, where y was the RFU difference or melting temperature and x was the proportion of *csr-1**, where x for unknown samples is estimated from

$$x = \frac{y - a}{B} \tag{1}$$

instead of fitting the proportion directly as a response. This allows fitting a normal distribution for the RFU difference or melting temperature, whereas proportion is constrained between 0 and 1. Thus, the Bayesian model for standard curve was:

$$\begin{aligned} y_i &\sim \mathrm{N}(\mu_i, \sigma) \\ \mu_i &= a + Bx_i \\ a, B &\sim \mathrm{N}(0, 10) \\ \sigma &\sim \mathrm{hC}(0, 2) \end{aligned} \tag{2}$$

where y_i was the ith observation of normalized RFU difference, x_i is the ith *csr-1** allele proportion, a is the intercept, and B is the slope is the standard curve. We used weakly regularizing (MCELREATH, 2015) gaussian priors for a and B, and half-cauchy (hC) prior for the standard deviation σ. For MCMC estimation we used two chains, with warmup set to 1000 followed by 3000 iterations for sampling. Convergence of the model was examined by using trace plots and $\hat{R}$ values, which were 1 for all estimated parameters. Proportion of unknown samples was estimated by using the posterior distributions for a and B and substituting them to equation 1. The values for proportion that were < 0 or > 1 were set to their limits. This way we obtained a posterior distribution for the *csr-1** allele proportion for each unknown sample.

Estimation of competitive fitness

Competitive fitness in haploid asexually reproducing organisms is just the ratio of growth rates of the competing types. Let N be population size, r growth rate, and t time, then population growth can be modeled as $N_t = (1+r)^t N_0$. If we have two competing types: A and B, then the proportions of these types grow as

$$\frac{A_t}{B_t} = \left(\frac{1+r_A}{1+r_B}\right)^t \frac{A_0}{B_0} = W_{AB}^t \left(\frac{A_0}{B_0}\right) \tag{3}$$

where W_{AB} is the fitness of type A relative to B. Taking a logarithm from equation 3 and substituting $B = 1 - A$ yields

$$\log\left(\frac{A_t}{1-A_t}\right) = \log\left(\frac{A_0}{1-A_0}\right) + \log(W_{AB}) \times t. \tag{4}$$

From this equation, we note that if we plot log-proportion of the two types against time, then $\log(W)$ is the slope of this line. This is the standard way to estimate competitive fitness in asexuals (HARTL and CLARK, 1997), and has been used extensively in the experimental evolution literature (LENSKI *et al.*, 1991). For *N. crassa*, this estimate works when strains are only allowed to reproduce asexually. We substitute the number of transfers for number of generations here; therefore, our fitness estimates include effects of mycelial growth rates and conidial production in as many cell divisions as it takes to go from spore to spore.

We included uncertainty in the *csr-1** allele proportion estimates in the model to estimate competitive fitness by using the observed posterior standard deviations for each *csr-1** allele proportion observation in the model (MCELREATH, 2015). To estimate relative fitnesses for the mating type and the *csr-1** allele, we fitted a model that accounted for competition, population effects, effect of

mating type, and the *csr-1** allele:

$$
\begin{aligned}
x_{est,i} &\sim \mathrm{N}(\mu_i, \sigma) \\
\log\left(\frac{\mu_i}{1-\mu_i}\right) &= \alpha_{comp[i]} + (\beta_{pop[i]} + \beta_{csr} + \beta_{matA} \times m_i) \times t_i \\
x_{obs,i} &\sim \mathrm{N}(x_{est,i}, x_{sd,i}) \\
\alpha_{comp[i]} &\sim \mathrm{N}(0, 0.065) \\
\beta_{pop[i]} &\sim \mathrm{N}(0, 1) \\
\beta_{csr}, \beta_{matA} &\sim \mathrm{N}(0, 1) \\
\sigma &\sim \mathrm{hC}(0, 2)
\end{aligned}
\tag{5}
$$

where $x_{obs,i}$ is the ith observed *csr-1** allele proportion, $x_{sd,i}$ is the observed error term for ith observation, $x_{est,i}$ is the estimated proportion for ith observation, $a_{comp[i]}$ is the intercept effect for each competition (four competitions), $\beta_{pop[i]}$ the slope effect of a replicate population (20 populations), β_{csr} is the effect of the *csr-1** allele, β_{matA} is the effect of mating type A, m_i is an indicator whether in ith observation the *csr-1** allele containing strain is mating type A, t_i is the transfer number for ith observation, and σ is the error standard deviation. Because these are competition experiments, where always two strains are competing, all the slope effects are relative effects, e.g. β_{matA} is the fitness effect of *mat A* relative to *mat a*. Therefore, the indicator $m_i \in \{-1, 0, 1\}$, so that $m_i = 1$ when *csr-1** allele containing strain is *mat A*, $m_i = -1$ when *csr-1** allele containing strain is *mat a*, and $m_i = 0$ when mating types are identical. This way we can use all information in the data to estimate the effect of *mat A* from all competitions. We used weakly regularizing priors for the β slope effects, and an informative prior for the intercept, α. Since we started the competition with spores of both strains at a frequency of 0.5, it makes sense to restrict intercept close to this value (0.5 is 0 on a logistic scale). The response of the model was fitted on the logistic scale, as at this scale relative fitness is the logarithm of the slope of this model, thus $W = \exp(\beta)$ for a given effect (Equation 4). MCMC estimation was done as above, but with 5000 iterations in total. Relative fitness of *mat A* and *csr-1** was calculated from posterior distributions of corresponding β effects.

When estimating the effect of the *qde-2* mutation, we first transformed the data such that the response indicated the frequency of the strain with the *qde-2* mutation and not necessarily the strain with the *csr-1** allele. The deterministic part of the model was:

$$\log\left(\frac{\mu_i}{1-\mu_i}\right) = \alpha_{comp[i]} + (\beta_{pop[i]} + \beta_{qde-2} + \beta_{csr} \times c_i + \beta_{matA} \times m_i) \times t_i \quad (6)$$

where β_{qde-2} is the effect of the *qde-2* mutation, β_{csr} is the effect of the *csr-1** allele, c_i is an indicator variable whether in ith observation the *qde-2* strain has the *csr-1** allele, $c_i \in \{-1, 1\}$, β_{matA} is the effect of mating type A, and m_i is an indicator variable whether in ith observation the *qde-2* strain is mating type A, $m_i \in \{-1, 1\}$. Neither the *csr-1** nor the mating type effect are ever absent; they are just present in different configurations in the different competitions. Other parameters, priors, and MCMC estimation were the same as above.

Since the two competition experiments have slightly different designs, but we wanted to use all possible information when estimating fitness effects for *mat A* and *csr-1**, we also combined their estimates from the two experiments meta-analytically. We used a model:

$$\begin{aligned} y_i &\sim \mathrm{N}(\mu_i, y_{sd,i}) \quad (7)\\ \mu_i &= \alpha \\ \alpha &\sim \mathrm{N}(0, 1) \end{aligned}$$

where y_i is the effect estimate, $y_{sd,i}$ is the observed error, and α is the meta-analytical estimate. Since there were only two experiments, we did not fit a term for experimental variation. Model was fit using the package 'brms' (BÜRKNER, 2017) with MCMC estimation as above, but with 4000 iterations in total.

Data availability

Strains will be available from the Fungal Genetics Stock Center (accession numbers pending). The data and scripts implementing all statistical analyses are available from the University of Jyväskylä

Digital Repository: https://doi.org/10.17011/jyx/dataset/65035

Results

Construction of marked strains

To introduce a marker to differentiate the strains in competition experiments, we modified the *csr-1* gene (ID: NCU00726) by homologous recombination. Rendering *csr-1* non-functional allows screening for positive transformants and distinguishing the strains by their *csr-1* sequences. After transformation we screened colonies for positive transformants; some of the colonies were heterokaryotic, but we found a homokaryotic transformant as well. We designated the new modified allele as *csr-1**. We subsequently validated the strains by Sanger sequencing, and observed the expected new *csr-1** and wild type *csr-1*$^+$ sequences in a positive transformant and the wild type, respectively. We crossed the *csr-1** marker to different genotypes to have strains with both mating types and in the *qde-2* mutant background (Table 1).

HRM assay optimization

To estimate the proportions of marked and unmarked conidia, we developed an HRM assay for the *csr-1* gene. We made mixtures with different proportions of *csr-1*$^+$ and *csr-1** conidia. We could distinguish samples containing different proportions of the two *csr* alleles based on their melting curves (Figure 2A). The calculated melting temperatures were 81 and 82.1 °C for the *csr-1** and wild type alleles, respectively. However, for the 50% mixture, the melting temperature in our assays was 81.9 °C, which is not the midpoint between these two temperatures (Figure 2B). The alleles investigated here have multiple changes, so formation of heteroduplex DNA has likely a large effect on melting curve shape. Attempts to make standard curves with the melting temperature also yielded unsatisfactory results. Therefore, we used the difference in the normalized RFU instead (Figure 2C), picking the temperature where the difference between proportions of 0 and 1 were maximized to have the highest dynamic range. Using the normalized difference, we obtained good

separation of the different proportions and a linear standard curve (Figure 2D).

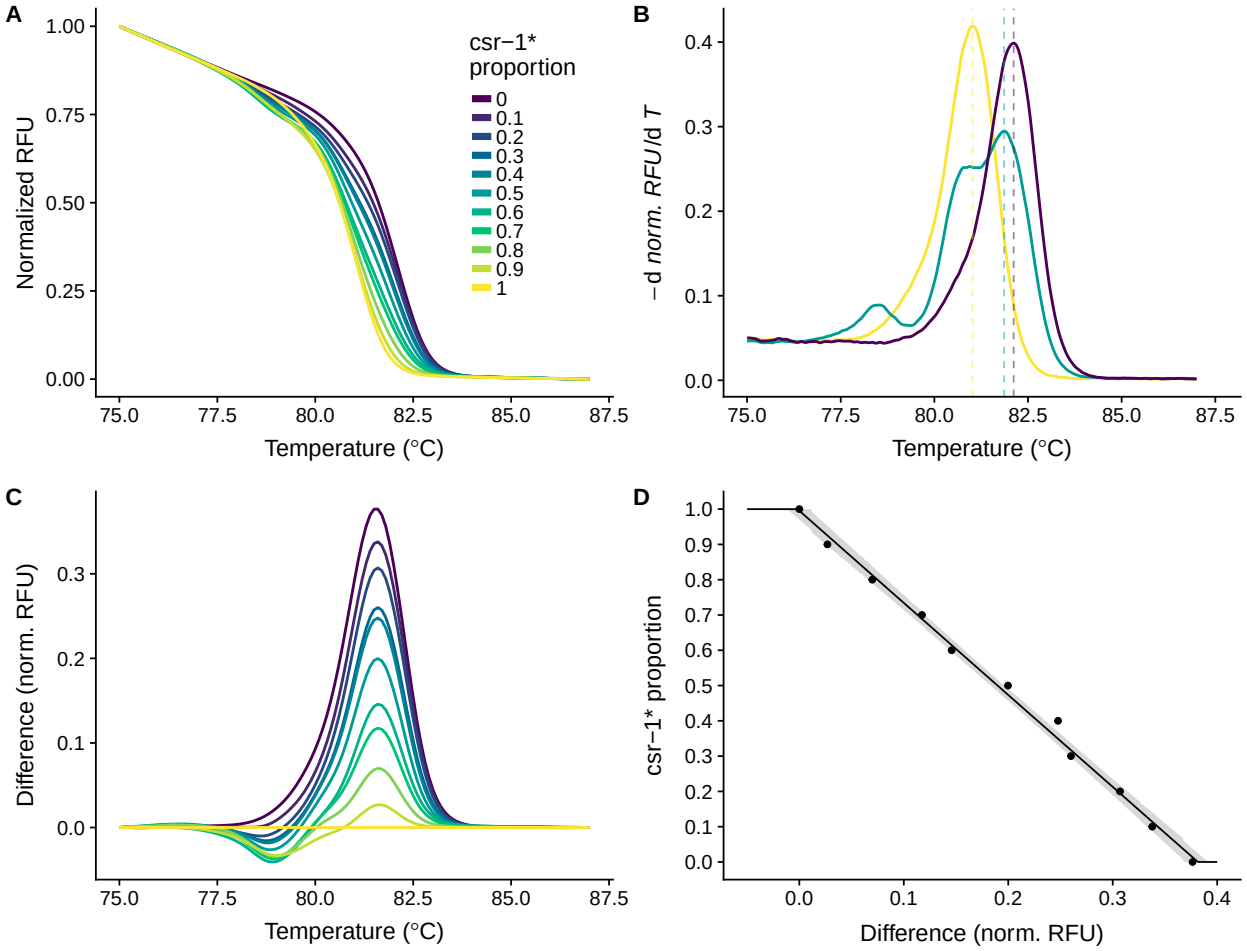

Figure 2: A) Melting curves of samples with different mixtures of *csr-1*$^{+}$ and *csr-1** conidia. Normalized fluorescence against temperature. B) Melting temperature, i.e. the inflection point of the melting curve, can be found at the maximum of the negative first derivative of normalized RFU. Negative derivative against temperature for samples with *csr-1** proportions of 1, 0.5, and 0. C) Difference curves for the melting curves in panel A, relative to *csr-1**. D) Standard curve for *csr-1** allele proportion in the sample and normalized RFU difference.

To assess the efficiency of the PCR reaction, we tested the effect of the number of conidia in DNA extractions on the real-time PCR reaction. We observed that C_q value decreased with increasing numbers of conidia in the DNA extraction (Figure S1). The slope of this relationship was -1.9 when using $\log_{10}$ transformed number of conidia, and no significant differences were observed for the two alleles; the alleles amplified with similar efficiency. There are likely some PCR inhibitors in the conidial DNA extraction as the slope is > -3.3. However, this is unlikely to

be a problem, since we are not interested in absolute quantification but we are interested in relative proportions always in one sample. Furthermore, the C_q values of competition experiment (see below) samples were similar; for the first competition experiment mean $C_q = 26.0$ and $\sigma = 0.63$, and for the second competition experiment mean $C_q = 25.8$ and $\sigma = 2.35$. The elevated standard deviation is due to a few samples having larger C_q values.

To summarize, the HRM assay allowed us to distinguish between *csr-1*$^+$ and *csr-1** alleles and to estimate the proportion of these alleles in unknown samples using known proportions as a standard curve (Figure 2D).

Competition experiments

Having a marker system that distinguishes strains from one another enabled us to perform competition experiments to estimate relative fitness of different genotypes. We inoculated two strains in one culture, and transferred conidia for three transfers and followed the strain frequencies using the HRM assay. This allowed us to estimate the relative fitness effects of different genotypes.

Effect of mating type and *csr-1** allele

In the first competition experiment, we tested the effect of the *csr-1** allele and the mating type of the strain. For the marker system to be useful, the marker itself should not have a large effect on fitness. We were also interested in the fitness effect of the mating type. When *N. crassa* mycelium grows, some hyphae fuse to form an interconnected network, which allows nutrient exchange within the mycelium. *N. crassa* strains that share the same mating type and heterocompatibility *het* alleles, such as the otherwise genetically identical strains used here, can fuse. Fusion is prevented for mycelia with different mating types (METZENBERG and GLASS, 1990). In our experiments, we observed that when strains shared the same mating type, and thus fused with each other, the frequency changes of the *csr-1** allele were much smaller than with opposite mating types (Figure 3). The *csr-1** allele had small frequency changes that seemed to go in both directions when mating types were the same (Figure 3A), indicating that the allele has no large fitness

effects. However, when mating types were different, and thus hyphal fusion was not possible, competitive exclusion seemed to happen quickly (Figure 3A). For the 2489 *mat a csr-1** vs. 2489 *mat A* competition, the marked strain won in two replicates while the unmarked strain won in three replicates (Figure 3A). In the 2489 *mat A csr-1** vs. 2489 *mat a* competition, the 2489 *mat a* always won. Overall this results in a broad estimate for the *mat A* fitness effect: W_{matA} = 0.63 (0.28–1.10, 95% HPDI) (Figure 3B). Since *mat A* strain won in some replicates in the other treatment, it seems likely that this is due to chance in a small sample of replicate populations. In the 2489 *mat A csr-1** vs. 2489 *mat A* competition, frequency changes were small. However, in the 2489 *mat a csr-1** vs. 2489 *mat a* competition there was an initial larger change in frequency after which the frequency changes were smaller (Figure 3A). The effect of *csr-1** allele on fitness was negative but the estimate overlapped with 1: W_{csr} = 0.72 (0.44–1.05, 95% HPDI). While the results suggest that there may be fitness effects, we cannot make final conclusions based on these results alone.

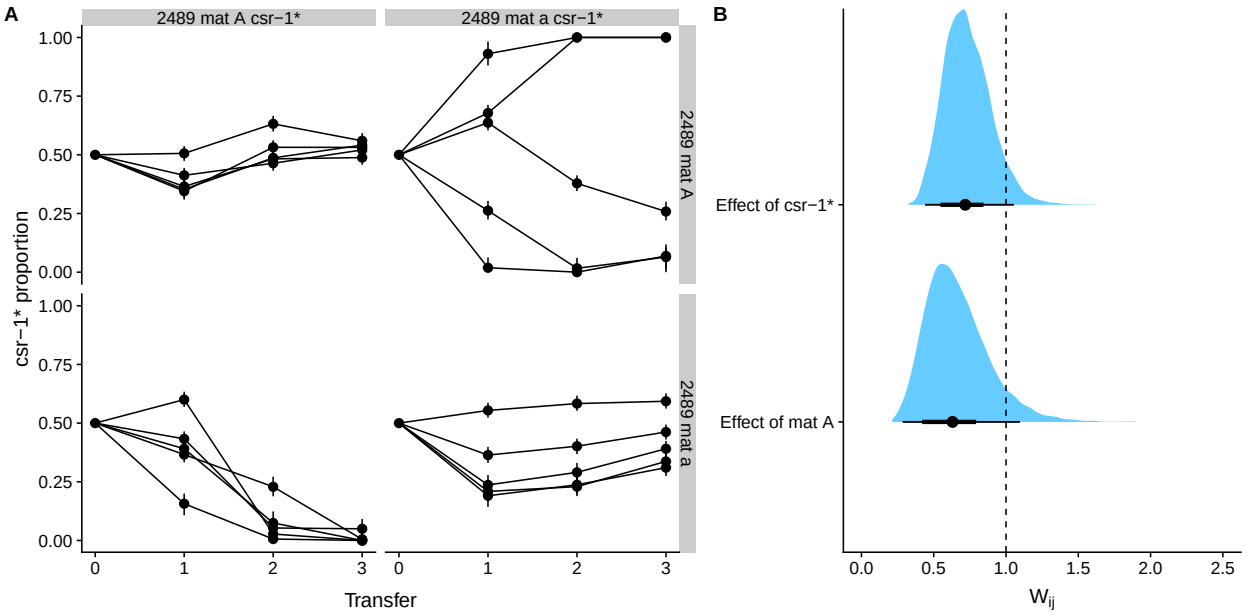

Figure 3: Results for the competition experiments testing the effect of the *csr-1** allele and mating type. For each treatment, $n = 5$ for a total of 20 populations. A) Frequency trajectories of the *csr-1** allele. B) Estimates of competitive fitness. Dots show point estimates for relative fitness, thick lines show the 66% and thin lines the 95% HPDI interval and the whole posterior distribution filled above. The dashed vertical line shows relative fitness of one, i.e. no difference.

Fitness effect of *qde-2* mutation

Next we estimated the fitness effect of the *qde-2* mutation with competition experiments. QDE-2 (ID: NCU04730) is the *N. crassa* ARGONAUTE homolog and the corresponding mutant is deficient in small RNA processing (MAITI *et al.*, 2007; LEE *et al.*, 2010). We had previously examined the effect of *qde-2* on growth in different environments (KRONHOLM *et al.*, 2016), and observed that it grows slower than the wild type. Therefore we expected that *qde-2* would have a lower relative fitness. Indeed, we observed that the strain with the *qde-2* mutation generally decreased in frequency (Figure 4A). In the 2489 *mat A* vs. 2489 *mat a csr-1**; Δ*qde-2* competition there was one population where the frequency of the *csr-1** allele initially decreased but then started to recover, this happened to a lesser extent for one population in the 2489 *mat A csr-1**; Δ*qde-2* vs. 2489 *mat a* competition as well (Figure 4A). The reason for this change of direction is unknown, one possibly is that a new beneficial mutation occurred in the *qde-2* background. Nevertheless, the *qde-2* strain clearly has a lower relative fitness compared to wild type (Figure 4B); the fitness estimate for *qde-2* was 0.30 (0.17–0.46, 95% HPDI). In this experiment, *mat A* had again a suggestive effect: 0.68 (0.41–1.04, 95% HPDI), but the estimate overlapped with one. However, if we combine the results of the two experiments meta-analytically the effect for mat A is different from one: 0.67 (0.46–0.94, 95% HPDI). There was no indication that the *csr-1** allele affected fitness in either this experiment (Figure 4B). When estimates were combined the effect of *csr-1** was 0.87 (0.64–1.18 95% HPDI). Together with results from the other competition experiment, *mat A* has a lower fitness than *mat a*, but importantly, the *csr-1** allele had no detectable effect on fitness.

Discussion

We showed that the *csr-1** allele can be used as a marker in competition experiments. The biological function of *csr-1* is not known, other than giving sensitivity to cyclosporin (BARDIYA and SHIU, 2007). As the *csr-1** is a nonfunctional allele of *csr-1*, the marker could potentially have some effect on fitness. However, both potential effect of the marker and a genotype of interest can be estimated

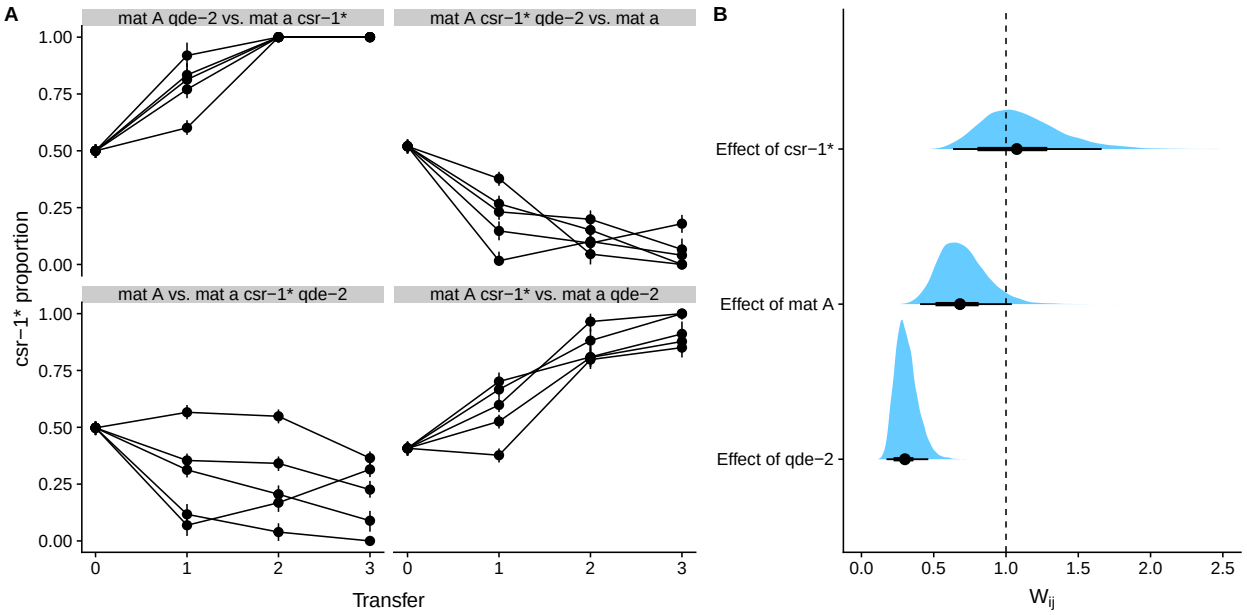

Figure 4: Results of competition experiments testing the effect of *qde-2* mutation. For each treatment, $n = 5$ for a total of 20 populations. A) Frequency trajectories of the *csr-1** allele. B) Estimates of competitive fitness effects for *qde-2* mutation relative to wild type, mating type A relative to mating type a, and *csr-1** relative to *csr-1*$^+$. Dots show point estimates for relative fitness, thick lines show the 66% and thin lines the 95% HPDI interval. The dashed vertical line shows relative fitness of one, i.e. no difference.

separately if the experimental design includes swapping the marker between the competing strains as done here. If swapping experiments are not possible, the known effect of the marker could be included in the model via priors. We detected no effect of *csr-1** on fitness in the laboratory environment used here, so the *csr-1** allele seems to be suitable as a marker for quantification of competitive fitness in *N. crassa*.

We also observed that when the two strains had the same mating type, the *csr-1** allele frequency changed only slowly or was maintained close to 0.5, but when strains of two different mating types were competing there seemed to be competitive exclusion of one of the strains. In *N. crassa*, genetically compatible strains undergo hyphal fusion only between strains that have the same mating type and compatible allorecognition alleles (METZENBERG and GLASS, 1990; ZHAO *et al.*, 2015). Since our strains are nearly isogenic, they can undergo hyphal fusion and form a heterokaryotic mycelium with respect to the *csr-1* locus, maintaining both alleles. This is what likely happened in competitions of strains with the same mating type. Nuclear ratios in *N. crassa* heterokaryons seem to be determined at the establishment phase of the heterokaryon, and the ratio of nuclei can be rather stable afterwards (ATWOOD and MUKAI, 1955; PITTENGER and ATWOOD, 1956). Frequency changes of different nuclei apparently require that the nuclei have different rates of mitosis, as diffusible components seem to be shared within the mycelium (PITTENGER and ATWOOD, 1956). In the related species *N. tetrasperma*, which has a pseudohomothallic mating system, there is some evidence that the different nuclei are maintained by active processes (SAMILS *et al.*, 2014). Furthermore, in the basidiomycete *Heterobasidion parviporum* ratios of different nuclei are affected by genetic and environmental effects (JAMES *et al.*, 2008).

In contrast, when strains with different mating types were competing, there seemed to be competitive exclusion, in which one strain often came to dominate the culture. When strains with different mating types fuse, cell death occurs in the fused cells, and these strains are thus unable to form heterokaryons (METZENBERG and GLASS, 1990), and competition must happen. Based on theoretical modeling of fungal fitness for a filamentous fungus life cycle in a system of many habitable patches, competitive exclusion between different strains is inevitable (GILCHRIST *et al.*,

2006). In our experiments, the strains were competing only for a single patch. In the laboratory, *N. crassa* seems to follow a bang-bang life history strategy (GILCHRIST *et al.*, 2006), where the mycelium first grows to cover nearby habitable area and then the fungus switches to spore production. Hence, our strains may be competing mainly for space in the culture tube. In some populations of the mating type and *csr-1** allele experiments, the mating type A seemed to win even if overall *mat a* had a higher fitness. In these cases, it may be that *mat A* gained some initial advantage due to chance, and thus gained an advantage by simply having more spores in the next transfer. During *N. crassa* spore germination as spore fusion increases growth (RICHARD *et al.*, 2012), a strain with more spores and thus more potential fusion partners may have an initial advantage even if its steady state growth rate of mature mycelium is slightly slower.

Surprisingly, when we combined information across experiments, we observed a fitness effect for the mating type locus with *mat a* having a higher relative fitness than *mat A*. In a facultative sexual species such as *N. crassa* both mating types have to be maintained in a population for sexual reproduction to occur; so it seems unexpected that one mating type has a higher asexual fitness than the other. However, it has been reported previously that in *N. crassa mat a* has a higher growth rate than *mat A* (RYAN *et al.*, 1943). Different mating types have been reported to have different growth rates also in other species: including *N. tetrasperma* (SAMILS *et al.*, 2014), *Pleurotus ostreatus* (LARRAYA *et al.*, 2001), and *Fusarium culmorum* (IRZYKOWSKA *et al.*, 2013). Considering that mating types can have differential fitness, how are they maintained in natural populations? One possibility is that the observed fitness advantage could be environmentally dependent, or alternatively, that sexual reproduction occurs often enough that mating type frequencies approach the evolutionary stable ratio of 1:1 despite differences in asexual fitness.

The *qde-2* mutation was known to grow slower than the wild type at 35 °C (KRONHOLM *et al.*, 2016), so the observation that it also has a lower competitive fitness is expected. Result showed that we can measure fitness effects of mutations with our marked strain system. The magnitude of the fitness effect is perhaps larger than expected: the growth rate of *qde-2* is 79% that of wild type at 35 °C (KRONHOLM *et al.*, 2016), while the relative fitness of *qde-2* was 30% that of wild

type. Thus, the relationship between mycelial growth rate and competitive fitness is not a simple one to one relationship. Similarly, large fitness effects, although with large uncertainty, were also observed for the *mat* locus. For example, the estimates seem large when compared to fitness effects of gene deletions in yeast (BELL, 2010). One possible explanation is that these estimates are not directly comparable as there is a large number of mitotic cell divisions between transfers, and one transfer from spore to spore in a filamentous fungus is not comparable to a cell division generation in unicellular yeasts or bacteria.

The *csr-1** allele is a very versatile marker. In this study, we used HRM PCR as a method to detect the proportion of the *csr-1** allele, but there are other methods to estimate *csr-1** allele proportion in a sample of spores. The simplest, although more laborious, method is to do replica plating of spores on plates with and without cyclosporine. Other PCR-based methods besides HRM that can detect the sequence difference between the *csr-1* alleles could also be used to estimate the proportion of the *csr-1**, such as digital droplet PCR with different probes (HINDSON *et al.*, 2011), pyrosequencing (HARRINGTON *et al.*, 2013), or any next generation sequencing technology, where many samples can be multiplexed with different barcodes and sequenced together (SMITH *et al.*, 2010). The advantage of our method is that it only requires to set up conventional PCR reactions taking little bench time, and the whole process can be done in 96-well plates enabling moderate throughput.

Another advantage of our method is the Bayesian model employed. Standard curves are commonly used in various biochemical assays, and while Bayesian approaches have been developed for various assays (GELMAN *et al.*, 2004; FENG *et al.*, 2010) they are rarely used in practise. Our model let's any uncertainty arising from the standard curve, the samples, or the initial inoculation via measuring proportion at transfer 0, to be propagated into the fitness estimates. Our modeling approach could also be used for other marker systems employing standard curves.

In conclusion, the marked strains reported here can be used to measure fitness effects of individual mutations or even for the fitness of strains derived by experimental evolution. They provide a versatile tool and advance the use of *N. crassa* as system studying experimental evolution and

ecology (LEE and DIGHTON, 2010; FISHER and LANG, 2016).

Acknowledgements

This study was supported by the Academy of Finland grant no. 274769 to IK and no. 278751 to TK. KJM was supported by National Institutes of Health Training Grant: T32 HD007348. EUS was supported by NIH grants GM093061 and GM127142. We thank Matthieu Bruneaux, Roghaieh Ashrafi, and Neda Moghadam for comments on the manuscript.

References

ANDERSON, J. L., B. P. S. NIEUWENHUIS, and H. JOHANNESSON, 2018 Asexual reproduction and growth rate: independent and plastic life history traits in *Neurospora crassa*. The ISME Journal **13**: 780–788.

ARANCIA, S., S. SANDINI, F. D. BERNARDIS, and D. FORTINI, 2011 Rapid, simple, and low-cost identification of *Candida* species using high-resolution melting analysis. Diagnostic Microbiology and Infectious Disease **69**: 283–285.

ASHRAFI, R., M. BRUNEAUX, L.-R. SUNDBERG, K. PULKKINEN, and T. KETOLA, 2017 Application of high resolution melting assay (HRM) to study temperature-dependent intraspecific competition in a pathogenic bacterium. Scientific Reports **7**: 980.

ATWOOD, K. C., and F. MUKAI, 1955 Nuclear distribution in conidia of *Neurospora* heterokaryons. Genetics **40**: 438–443.

BARDIYA, N., and P. K. SHIU, 2007 Cyclosporin A-resistance based gene placement system for *Neurospora crassa*. Fungal Genetics and Biology **44**: 307–314.

BASTIAANS, E., A. J. M. DEBETS, and D. K. AANEN, 2016 Experimental evolution reveals that high relatedness protects multicellular cooperation from cheaters. Nat Commun **7**: 11435.

BELL, G., 2010 Experimental genomics of fitness in yeast. Proceedings of the Royal Society B: Biological Sciences **277**: 1459–1467.

BÜRKNER, P.-C., 2017 brms: An R package for Bayesian multilevel models using Stan. Journal of Statistical Software, Articles **80**: 1–28.

CARPENTER, B., A. GELMAN, M. HOFFMAN, D. LEE, B. GOODRICH, *et al.*, 2017 Stan: A probabilistic programming language. Journal of Statistical Software **76**: 1–32.

COLOT, H. V., G. PARK, G. E. TURNER, C. RINGELBERG, C. M. CREW, *et al.*, 2006 A high-throughput gene knockout procedure for *Neurospora* reveals functions for multiple transcription factors. Proceedings of the National Academy of Sciences **103**: 10352–10357.

DAVIS, R. H., and F. J. DE SERRES, 1970 Genetic and microbiological research techniques for *Neurospora crassa*. Methods in Enzymology **17**: 79–143.

FENG, F., A. P. SALES, and T. B. KEPLER, 2010 A Bayesian approach for estimating calibration curves and unknown concentrations in immunoassays. Bioinformatics **27**: 707–712.

FISHER, K. J., and G. I. LANG, 2016 Experimental evolution in fungi: An untapped resource. Fungal Genetics and Biology **94**: 88–94.

FREITAG, M., P. C. HICKEY, N. B. RAJU, E. U. SELKER, and N. D. READ, 2004 GFP as a tool to analyze the organization, dynamics and function of nuclei and microtubules in *Neurospora crassa*. Fungal Genetics and Biology **41**: 897–910.

GELMAN, A., G. L. CHEW, and M. SHNAIDMAN, 2004 Bayesian analysis of serial dilution assays. Biometrics **60**: 407–417.

GILCHRIST, M. A., D. L. SULSKY, and A. PRINGLE, 2006 Identifying fitness and optimal life-history strategies for an asexual filamentous fungus. Evolution **60**: 970–979.

GRAHAM, J. K., M. L. SMITH, and A. M. SIMONS, 2014 Experimental evolution of bet hedging under manipulated environmental uncertainty in *Neurospora crassa*. Proceedings of the Royal Society B: Biological Sciences **281**: 20140706.

HARRINGTON, C. T., E. I. LIN, M. T. OLSON, and J. R. ESHLEMAN, 2013 Fundamentals of pyrosequencing. Archives of Pathology & Laboratory Medicine **137**: 1296–1303. PMID: 23991743.

HARTL, D. L., and A. G. CLARK, 1997 *Principles of Population Genetics*. Sinauer Associates, Inc., Sunderland, 3rd edition.

HINDSON, B. J., K. D. NESS, D. A. MASQUELIER, P. BELGRADER, N. J. HEREDIA, *et al.*, 2011 High-throughput droplet digital PCR system for absolute quantitation of DNA copy number. Analytical Chemistry **83**: 8604–8610. PMID: 22035192.

IRZYKOWSKA, L., J. BOCIANOWSKI, and A. BATURO-CIEŚNIEWSKA, 2013 Association of mating-type with mycelium growth rate and genetic variability of *Fusarium culmorum*. Central European Journal of Biology **8**: 701–711.

JAMES, T. Y., J. STENLID, Å. OLSON, and H. JOHANNESSON, 2008 Evolutionary significance of imbalanced nuclear ratios within heterokaryons of the basidiomycete fungus *Heterobasidion Parviporum*. Evolution **62**: 2279–2296.

KRONHOLM, I., H. JOHANNESSON, and T. KETOLA, 2016 Epigenetic control of phenotypic plasticity in the filamentous fungus *Neurospora crassa*. G3: Genes|Genomes|Genetics **6**: 4009–4022.

LARRAYA, L. M., G. PÉREZ, I. IRIBARREN, J. A. BLANCO, M. ALFONSO, *et al.*, 2001 Relationship between monokaryotic growth rate and mating type in the edible basidiomycete *Pleurotus ostreatus*. Applied and Environmental Microbiology **67**: 3385–3390.

LEE, H.-C., L. LI, W. GU, Z. XUE, S. K. CROSTHWAITE, *et al.*, 2010 Diverse pathways generate microRNA-like RNAs and Dicer-independent small interfering RNAs in fungi. Molecular Cell **38**: 803–814.

LEE, K., and J. DIGHTON, 2010 *Neurospora*, a potential fungal organism for experimental and evolutionary ecology. Fungal Biology Reviews **24**: 85–89.

LENSKI, R. E., J. A. MONGOLD, P. D. SNIEGOWSKI, M. TRAVISANO, F. VASI, *et al.*, 1998 Evolution of competitive fitness in experimental populations of *E. coli*: What makes one genotype better competitor than another? Antonie van Leeuwenhoek **73**: 35–47.

LENSKI, R. E., M. R. ROSE, S. C. SIMPSON, and S. C. TADLER, 1991 Long-term experimental evolution in *Escherichia coli*. I. Adaptation and divergence during 2,000 generations. American Naturalist **138**: 1315–1341.

MAITI, M., H.-C. LEE, and Y. LIU, 2007 QIP, a putative exonuclease, interacts with the *Neurospora* Argonaute protein and facilitates conversion of duplex siRNA into single strands. Genes Dev **21**: 590–600.

MARGOLIN, B. S., M. FREITAG, and E. U. SELKER, 1997 Improved plasmids for gene targeting at the *his-3* locus of *Neurospora crassa* by electroporation. Fungal Genetics Newsletter **44**: 34–36.

MCCLUSKEY, K., A. WIEST, and M. PLAMANN, 2010 The fungal genetics stock center: a repository for 50 years of fungal genetics research. J Biosci **35**: 119–126.

MCELREATH, R., 2015 *Statistical Rethinking - A Bayesian course for with examples in R and Stan*. CRC Press, New York.

METZENBERG, R. L., 2003 Vogel's medium N salts: Avoiding the need for ammonium nitrate. Fungal Genetics Newsletter **50**: 14.

METZENBERG, R. L., and N. L. GLASS, 1990 Mating type and mating strategies in *Neurospora*. BioEssays **12**: 53–59.

554 MEUNIER, C., S. HOSSEINI, N. HEIDARI, Z. MARYUSH, and H. JOHANNESSON, 2018 Multi-level selection in the filamentous ascomycete *Neurospora tetrasperma*. The American Naturalist 556 **191**: 290–305.

NINOMIYA, Y., K. SUZUKI, C. ISHII, and H. INOUE, 2004 Highly efficient gene replacements 558 in *Neurospora* strains deficient for non-homologous end-joining. Proceedings of the National Academy of Sciences **101**: 12248–12253.

560 OAKLEY, C. E., C. L. WEIL, P. L. KRETZ, and B. R. OAKLEY, 1987 Cloning of the *riboB* locus of *Aspergillus nidulans*. Gene **53**: 293–298.

562 PITTENGER, T., and K. C. ATWOOD, 1956 Stability of nuclear proportions during growth of *Neurospora* heterokaryons. Genetics **41**: 227–241.

564 PRINGLE, A., and J. W. TAYLOR, 2002 The fitness of filamentous fungi. Trends in Microbiology **10**: 474–481.

566 R CORE TEAM, 2018 *R: A language and environment for statistical computing*. R Foundation for Statistical Computing, Vienna, Austria.

568 RICHARD, F., N. L. GLASS, and A. PRINGLE, 2012 Cooperation among germinating spores facilitates the growth of the fungus, *Neurospora crassa*. Biology Letters **8**: 419–422.

570 ROCHE, C. M., J. J. LOROS, K. MCCLUSKEY, and N. L. GLASS, 2014 *Neurospora crassa*: looking back and looking forward at a model microbe. Am J Bot **101**: 2022–2035.

572 ROMERO-OLIVARES, A. L., J. W. TAYLOR, and K. K. TRESEDER, 2015 *Neurospora discreta* as a model to assess adaptation of soil fungi to warming. BMC Evol Biol **15**: 198.

574 RYAN, F. J., G. W. BEADLE, and E. L. TATUM, 1943 The tube method of measuring the growth rate of *Neurospora*. American Journal of Botany **30**: 784–799.

576 SAMILS, N., J. OLIVA, and H. JOHANNESSON, 2014 Nuclear interactions in a heterokaryon: insight from the model *Neurospora tetrasperma*. Proceedings of the Royal Society B: Biological
578 Sciences **281**: 20140084.

SCHOUSTRA, S. E., M. SLAKHORST, A. J. M. DEBETS, and R. F. HOEKSTRA, 2005 Comparing
580 artificial and natural selection in rate of adaptation to genetic stress in *Aspergillus nidulans*. Journal of Evolutionary Biology **18**: 771–778.

582 SMITH, A. M., L. E. HEISLER, R. P. ST.ONGE, E. FARIAS-HESSON, I. M. WALLACE, *et al.*, 2010 Highly-multiplexed barcode sequencing: an efficient method for parallel analysis of pooled
584 samples. Nucleic Acids Research **38**: e142–e142.

WICKHAM, H., 2016 *ggplot2: Elegant Graphics for Data Analysis*. Springer-Verlag New York.

586 WITTWER, C. T., G. H. REED, C. N. GUNDRY, J. G. VANDERSTEEN, and R. J. PRYOR, 2003 High-resolution genotyping by amplicon melting analysis using LCGreen. Clinical Chemistry
588 **49**: 853–860.

WOJDACZ, T. K., and A. DOBROVIC, 2007 Methylation-sensitive high resolution melting (MS-
590 HRM): a new approach for sensitive and high-throughput assessment of methylation. Nucleic Acids Research **35**: e41.

592 ZHAO, J., P. GLADIEUX, E. HUTCHISON, J. BUECHE, C. HALL, *et al.*, 2015 Identification of allorecognition loci in *Neurospora crassa* by genomics and evolutionary approaches. Molecular
594 Biology and Evolution **32**: 2417–2432.

Supplementary Information

Supplementary Figures

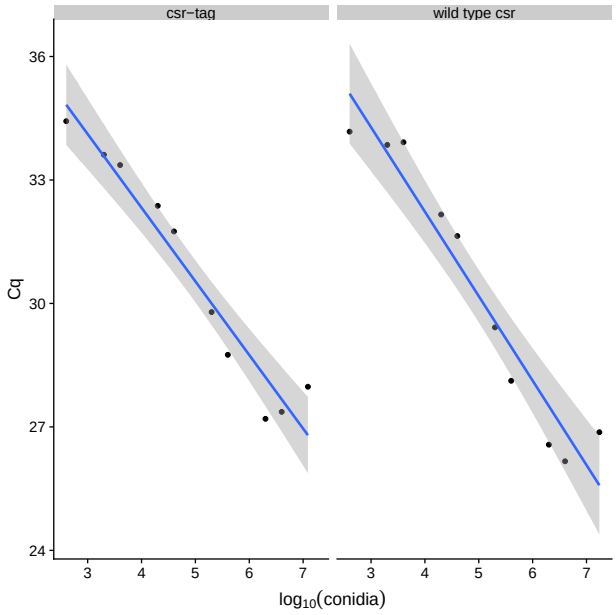

Figure S1: Correlation between number of conidia used in DNA extraction (log-scale) and number of PCR cycles required to detect the PCR-product. Differences between the alleles are not significant.

Supplementary Tables

Table S1: Primers used in the study.

Name	Sequence
csrL-f	TGC CAT GTT CTT CTT GAG CC
csrL-r	CCC ATG TTT GCG CGG ACC TGG AGA AGC GGC TGG ACT TAC ACT ATT ACA TGA ATT CGG ATG TTT GCG AAA AAG CTC TGG
csrR-f	CAC TGC AAC TTT CTC CTG CGC CAG AGC TTT TTC GCA AAC ATC CGA ATT CAT GTA ATA GTG TAA GTC CAG CCG CTT CTC
csrR-r	GAC AAT GGT GGG CTT CTT GG
csr-hrm-f	CGT CAT CTC TCA AGC CCA CT
csr-hrm-r	GAG AAG CGG CTG GAC TTA CA